EurJIC European Journal of Inorganic Chemistry

FULL PAPER

DOI: 10.1002/ejic.201101201

Supramolecular Adducts of Negatively Charged Lanthanide(III) DOTP Chelates and Cyclodextrins Functionalized with Ammonium Groups: Mass Spectrometry and Nuclear Magnetic Resonance Studies

Giovannia A. Pereira,[a][‡] Joop A. Peters,[b] Enzo Terreno,[c] Daniela Delli Castelli,[c] Silvio Aime,[c] Sophie Laurent,[d] Luce Vander Elst,[d] Robert N. Muller,[d] and Carlos F. G. C. Geraldes*[a]

Keywords: Lanthanides / Imaging agents / Supramolecular chemistry / NMR spectroscopy / Mass spectrometry

The interaction of the negatively charged Ln^{3+} chelate Ln–DOTP with β- and γ-cyclodextrins bearing ammonium groups at the upper rim (CD^+s) was investigated using mass spectrometry and NMR spectroscopic techniques. Mass spectroscopy shows the presence of 1:1 adducts of Ln–DOTP and both β- or γ-CD^+. The peak intensities increased upon increasing the pH of the samples from 7 to 9.0, suggesting an increase in the strength of the interaction. Lanthanide induced ^1H NMR chemical shifts and relaxation rates measured in aqueous solutions confirmed the presence of these adducts. The strength of the interactions appeared to be dependent on the pH, reflecting the strong electrostatic interactions between the oppositely charged host CD^+ and guest Ln–DOTP chelate. Evaluation of the lanthanide induced relaxation rates showed that the Ln–DOTP does not enter the cavity of the CDs, but remains above it with a distance of 10–11 Å between the Ln^{3+} ion and the centre of the CD. Molecular modelling indicated that hydrogen bonds between the functionalized groups participating in the interaction sites contribute to the adduct stabilization. The apparent binding constants at pH 7 and 9 were obtained by using relaxometric measurements at 9 MHz. Fitting the NMRD profiles showed an increase in the number of second-sphere water molecules surrounding the phosphonate pendant arms of the Ln–DOTP chelate upon its interaction with the CDs. A brief description of the PARACEST properties of the supramolecular systems formed by Tm–DOTP and the positively charged CDs is presented. Both CDs display a shift of the saturation transfer peaks of the ammonium functions by the Tm complex, with an accentuated effect observed for the γ-CD derivative.

Introduction

Gd^{3+} complexes are commonly used in clinical diagnostics such as magnetic resonance imaging (MRI) contrast agents (CAs), because of their high paramagnetism ($4f^7$ electronic configuration) and long electron spin relaxation times of the metal centre.[1–5] The contrast enhancement depends on the ability of the CA to selectively enhance the relaxation times of water protons of different tissues. This enhancement results from a dipolar interaction between the large electronic magnetic moment of the Gd^{3+} ion and the magnetic moments of the water protons in its vicinity. The efficacy is expressed by means of the relaxivity (r_i, i = 1, 2), which represents the relaxation rate enhancement of water protons in solutions containing the paramagnetic agent standardized at 1 mM Gd^{3+}. Besides the number of water molecules in the inner coordination sphere, the relaxivity of a Gd^{3+} complex is determined by the various correlation times modulating the dipolar interaction. It has been recognized that high relaxivities at the common imaging fields (0.5–1.5 T) may be obtained for long rotational correlation times (τ_R) and electronic spin relaxation times (T_{1e}) and a short lifetime of the water molecules in the first coordination sphere of Gd^{3+} (τ_M).[1–5]

Thus, an approach to optimize the efficacy of CAs is to increase τ_R by increasing the size of the paramagnetic complex. This has been attained either by covalent binding of Gd^{3+} chelates to slowly tumbling macro(bio)molecules (linear polymers,[6] carbohydrates,[7] proteins[8] and dendrimers[9]) or through noncovalent binding of a suitably functionalized Gd^{3+} complex to macromolecules, usually human serum albumin.[8a,10] Alternative ways to achieve this goal are through self-assembly of Gd^{3+} chelates,[11] such as

[a] Department of Life Sciences and Center of Neurosciences and Cell Biology, Faculty of Science and Technology, University of Coimbra,
P. O. Box 3046, 3001-401 Coimbra, Portugal
Fax: +351-239853607
E-mail: geraldes@ci.uc.pt
[b] Biocatalysis and Organic Chemistry, Department of Biotechnology, Delft University of Technology,
Julianalaan 136, 2628 BL Delft, The Netherlands
[c] Department of Chemistry, University of Torino,
via P. Giuria 7, 10125 Torino, Italy
[d] Department of General, Organic and Biomedical Chemistry, NMR and Molecular Imaging Laboratory, University of Mons,
7000 Mons, Belgium
[‡] Present address: Departamento de Química Fundamental, Universidade Federal de Pernambuco,
50740-560 Recife, Pernambuco, Brasil

amphiphilic ones[12] or through the inclusion of lipophilic Gd^{3+} chelates in liposomes[13] or other lipid-based colloidal systems.[14]

The cylodextrins have been used as scaffolds for the covalent attachment of Ln^{3+} ions or Ln^{3+} complexes as luminescent probes or slowly rotating Gd^{3+}-based MRI agents.[15] The formation of supramolecular structures by inclusion of Gd^{3+} chelates in cyclodextrins is yet another way to attain slow rotational dynamics in solution. The cyclodextrins (CDs) are a family of cone-shaped, cyclic oligosaccharides consisting of six (α-CD), seven (β-CD) or eight (γ-CD) α(1–4)-interconnected D-glucose units. The external surface of the CD cones is hydrophilic, while the internal surface is relatively hydrophobic, as none of the hydroxy groups point towards the interior of the cavity. The primary $C_{(6)}H_2OH$ groups of the glucose units are at the narrow rim, while the secondary $C_{(2)}HOH$ and $C_{(3)}HOH$ groups are at the wide one. They readily form inclusion complexes with guest molecules of suitable size, shape and polarity. As a general rule, the complex is strong when there is size complementarity between the guest and the cavity of the CDs, which have internal diameters of 4.7–5.2, 6.0–6.5 and 7.5–8.5 Å, for the α-, β- and γ-CDs, respectively. Such host–guest inclusion complexes are used in a variety of industrial[16,17] and pharmaceutical applications.[18] Many NMR spectroscopic studies have been published on the solution structure and the thermodynamic stability of host–guest compounds of CDs with organic molecules.[19,20] Inclusion complexes of γ-CDs with crown ethers, azamacrocycles and their complexes with metal cations (Li^+, Ca^{2+}, Ba^{2+}) have been characterized.[21–23]

Among the unsubstituted CDs, only the γ-CD interacts in aqueous solution with Gd^{3+} chelates of unsubstituted tetraazamacrocyclic ligands, like Gd–DOTA and Gd–DOTP [H_4DOTA = DOTA = 1,4,7,10-tetraazacyclododecane-1,4,7,10-tetraacetic acid, H_8DOTP = 1,4,7,10-tetraazacyclododecane-1,4,7,10-tetrakis(methylenephosphonic acid), see Figure 1].[24,25] However, these interactions are quite weak, as these macrocyclic chelates are somewhat too large to perfectly fit into the cavity of the widest cyclodextrin, γ-CD.[26] More stable inclusion compounds and supramolecular assemblies have been obtained with Gd–DOTA or Gd–DTPA (H_5DTPA = diethylenetriaminetetraacetic acid) complexes bearing hydrophobic substituents of the appropriate size and β-CD.[10c,27–29]

Modified charged cyclodextrins, such as mono- or peraminated β-CDs, have been found to be capable of chiral recognition, e.g. of α-amino acids, through a combination of coulombic interactions and inclusion.[30,31] These modified CDs are also cone-shaped with a hydrophobic cavity, which is however more expanded in an aqueous medium due to the strong electrostatic repulsions between the charged substituents.

Here, we report the results of a study aimed at increasing the strength of the interaction between the negatively charged Gd–DOTP and the CDs by means of substitution of the upper rim of the latter with positively charged ammonium groups. The positively charged CDs will be represented as β-CD^+ and γ-CD^+, respectively (see Figure 1). Mass spectrometry (MS) experiments[32–34] were used to verify the existence of noncovalent interactions between the negatively charged chelates and the CD^+s and to determine the stoichiometry of the adducts. The stability and the structures of the supramolecular systems formed were studied in more detail by ^1H and ^{31}P NMR spectroscopy, and water ^1H relaxometry and longitudinal ^1H nuclear magnetic resonance dispersion (NMRD) techniques. Additionally, the PARACEST properties of these supramolecular compounds were also evaluated.[35]

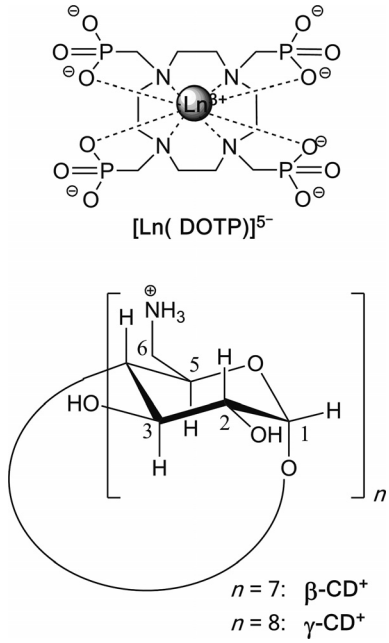

Figure 1. Chemical structures of the interacting systems discussed, Ln–DOTP, β- and γ-CD^+.

Results and Discussion

The modified (β,γ)-CD^+s have seven or eight amino groups with pK_a values ranging from 6.9 to 8.5,[36] thus they are positively charged over a large pH range. The pK_a values reported for the $[Ln(DOTP)]^{5-}$ complex are in the range 4.4–7.9.[37] Since the NMR spectroscopic study was carried out at pH 7–9, the CD^+s and the Ln–DOTP are present as partially protonated cationic and anionic forms, respectively, under the present conditions. The exact protonation state of the Ln–DOTP complex will depend on the pH and may be influenced by supermolecular interactions. For the sake of simplicity these chelates are denoted as Ln–DOTP, irrespective of the protonation state and the charge.

Mass Spectrometry

Thanks to its very high sensitivity mass spectrometry has become an important tool in the investigation of supramolecular systems. Here we exploit this technique to verify the existence of adducts of the CD^+s and the Ln^{3+} chelates

and to determine their stoichiometries. The mass spectrum obtained for an equimolar mixture (ρ = 1, ρ = [Ln^{3+}–chelate]/[cyclodextrin]) of β-CD^+ and Gd–DOTP at pH 7.0 (Figure 2) shows the signals of β-CD^+ at *m*/*z* = 1128 ([β-CD^+ + H]$^+$) and 1150 ([β-CD^+ + Na]$^+$) and those for the Gd–DOTP at *m*/*z* = 725 ([Gd(DOTP) + Na]$^+$) and 747 ([Gd(DOTP) + 2Na]$^+$). In addition signals were observed at *m*/*z* = 916 ([β-CD^+ + Gd(DOTP) + 2H]$^{2+}$), *m*/*z* = 928 ([β-CD^+ + Gd(DOTP) + H + Na]$^{2+}$), *m*/*z* = 938 ([β-CD^+ + Gd(DOTP) + 2Na]$^{2+}$), *m*/*z* = 960 ([β-CD^+ + Gd(DOTP) + 4Na]$^{2+}$) and *m*/*z* = 971 ([β-CD^+ + Gd(DOTP) + 5Na]$^{2+}$). The mass spectrum at pH 9.0 (Figure 2) is very similar to that at pH 7.0, except for the higher signal intensities of the 1:1 adduct relative to those of the free cyclodextrin, specially for the *m*/*z* = 916 signal. Similar mass spectra were obtained for an equimolar mixture of γ-CD^+ and Gd–

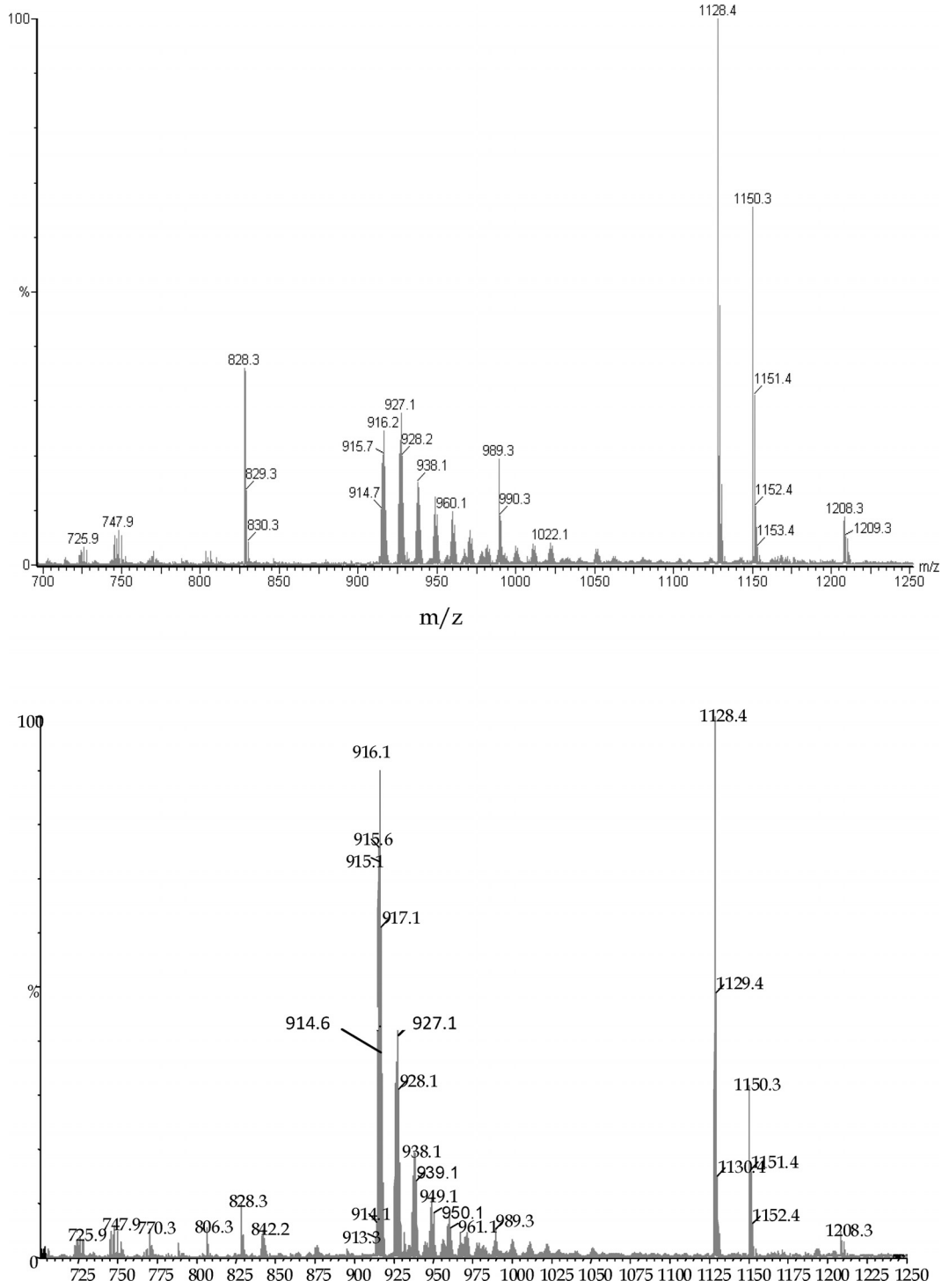

Figure 2. Mass spectrum of β-CD^+ + Gd–DOTP, ρ = 1, at pH 9.0 (bottom) and pH 7.0 (top).

DOTP at pH 7.0 and 9.0 (Figure S1). These data indicate that both β- and γ-CD^+ form a 1:1 noncovalent adduct with Gd–DOTP, and the effect of the pH on the peak intensities suggests that the supramolecular interaction at pH 9.0 is stronger than at pH 7. This can be explained by the increased Coulomb interaction from the increase of the negative charge of the Gd–DOTP species as a result of the deprotonation.

^{31}P NMR and ^{1}H NMR Chemical Shifts as a Function of ρ

The interaction of the two positively charged aminated cyclodextrins, β-CD^+ and γ-CD^+, by titration with the negatively charged Ln–DOTP was investigated for Ln = Nd and Tm. Qualitatively, very similar phenomena were observed, although the lanthanide-induced shifts were obviously different for the two lanthanides. Here, we discuss only the spectra for the Nd^{3+} complex, the spectra for Tm^{3+} are displayed in the Supporting Information. The spectra were assigned by comparison with those of the β- and γ-CD^+s and the free Ln^{3+}–chelates.

The X-ray crystal structure of Gd–DOTP shows an eight-coordinate Gd^{3+} ion bound to the ligand, with a twisted square antiprismatic (TSAP or m′) conformation, with no inner-sphere water. This TSAP isomer appears in the crystal as a racemic mixture of enantiomers, Λ(λλλλ) and Δ(δδδδ).[38] In solution, the Ln–DOTP complexes also exist as a racemic mixture of these two enantiomers, which are obviously indistinguishable by NMR spectroscopy.[39]

The supramolecular interaction between β-CD^+ and Nd–DOTP was followed by ^{31}P NMR spectroscopy upon addition of increasing concentrations (ρ = 0–5) of Nd–DOTP to a 5 mM solution of β-CD^+ at pH 7 (see Figure 3). At ρ = 0.25, a single ^{31}P NMR resonance was observed at δ =

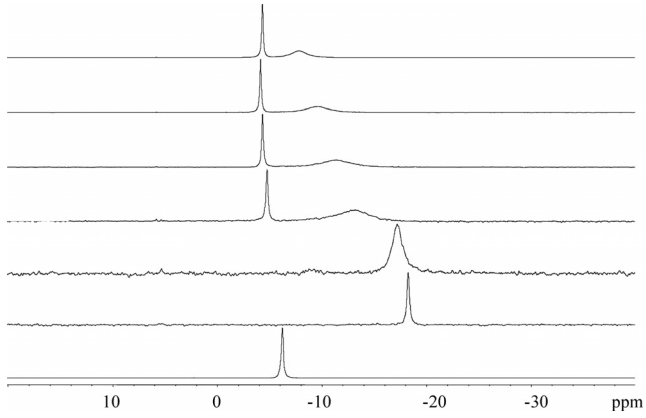

Figure 3. ^{31}P NMR titration (202.274 MHz) of the β-CD^+ with Nd–DOTP in D_2O, pH 9.0, 298 K. Bottom to top: Nd(DOTP) 12.5 mM, ρ = 0.25, 0.5, 1.0, 1.5, 2.5, 5.0.

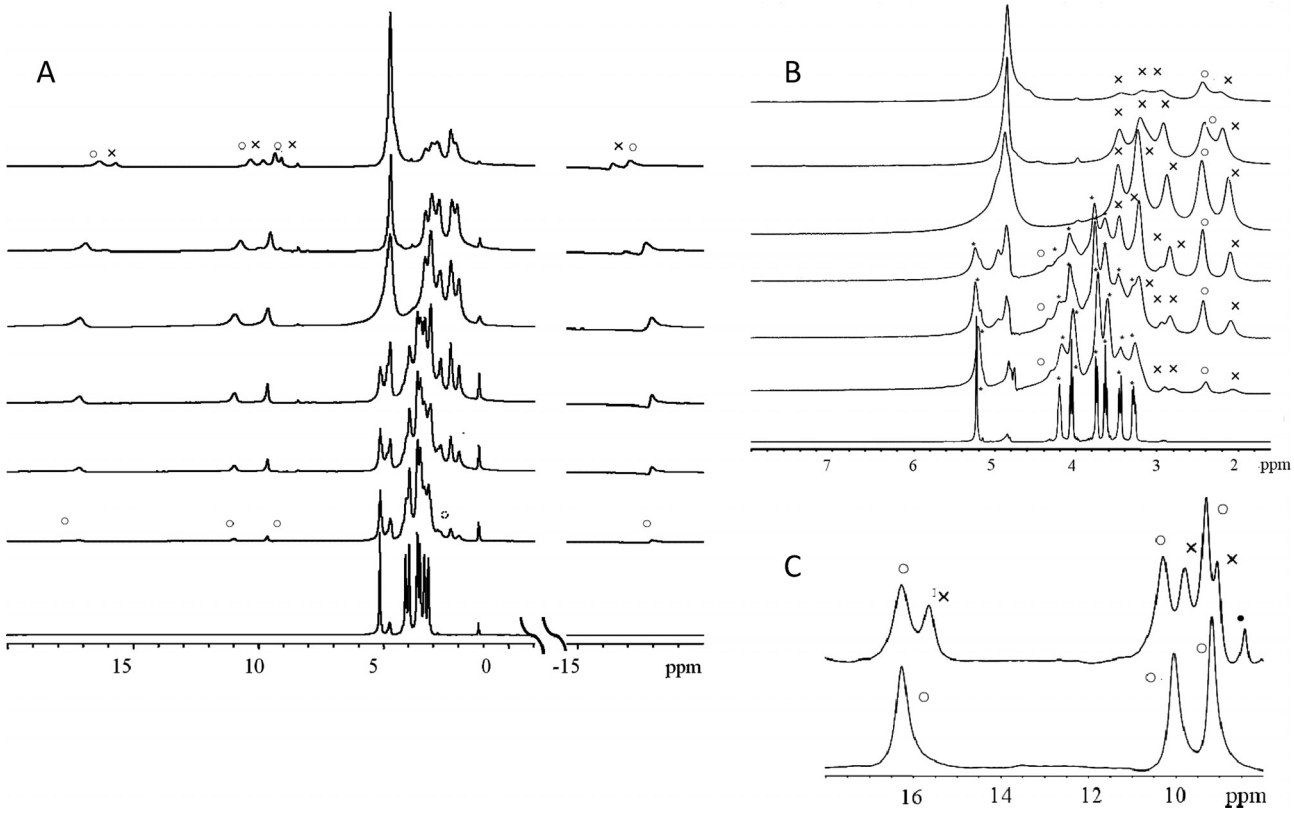

Figure 4. (A) ^{1}H NMR spectra of 5 mM β-CD^+ in the presence of increasing concentrations of Nd–DOTP in D_2O, (pH 7.0, 298 K and 500 MHz); (B) Expansion of the diamagnetic region with some of the Nd–DOTP resonances; (C) Expansion showing the H1, H5 and H6 protons of 25 mM Nd–DOTP (bottom) and a mixture of Nd–DOTP and β-CD^+ (ρ = 5) (top). Peaks of β-CD^+, bound Nd–DOTP and free Nd–DOTP are labelled with *, ×, ○, respectively.

–18 ppm at pH 9, which can be assigned to the 1:1 adduct. At $\rho > 0.5$, a resonance for free Nd–DOTP appeared at about –6 ppm. Upon further increase of ρ, the resonance for the adduct showed broadening and at the same time it shifted downfield. This suggests an interaction between the 1:1 adduct and Nd–DOTP. Although this adduct is diastereomeric, no splitting of the resonances was observed. Apparently, the exchange between the Λ(λλλλ) and Δ(δδδδ) CD^+-Nd–DOTP adducts is either fast on the ^{31}P NMR shift timescale or the chemical shift difference between them is unobservable.

Similar phenomena were observed in the ^1H NMR spectra of these samples (Figure 4). Upon increase of ρ, increased broadening and induced shifts were observed for the resonances for β-CD^+, while two new sets of resonances appeared. One of these sets had the same chemical shifts as that of a sample of free Nd–DOTP and the position of the signals in the other set was close to those of the resonances for free Nd–DOTP. Therefore, these signals were assigned to the DOTP part of the 1:1 adduct. The relative intensities of the resonances were in agreement with this assignment. These phenomena indicate that the exchange of the DOTP resonances between the free form and the adduct is slow on the ^1H NMR shift timescale, whereas the corresponding exchange of the β-CD^+ resonances is in the rapid-exchange regime, although with substantial exchange broadening. It cannot be excluded that this broadening is caused by binding of a second Nd–DOTP to the β-CD^+ (M_2L complex).

A similar ^1H NMR spectroscopic titration experiment carried out with γ-CD^+ and Nd–DOTP led to similar results (Figure S2). Once again, the signals of the two diastereomers of the adduct were not resolved.

pH Dependence of the ^{31}P NMR Chemical Shifts

As an example, Figure 5 displays the pH dependence of the ^{31}P NMR chemical shifts for a sample of β-CD^+ and Nd–DOTP at $\rho = 1$ and 298 K. Between pH 5 and 7, a single resonance is observed at $\delta = -21$ ppm. In this pH region β-CD^+ is fully protonated and this resonance can be assigned to the 1:1 adduct of this species with the Nd–DOTP complex. Between pH 7 and 9 the resonance moves to about –8 ppm. At the same time a resonance for free Nd–DOTP appears at $\delta = -9$ ppm, which shifts to –5.2 for this pH trajectory. The jumps in both resonances can be ascribed to deprotonation. Upon increase of the pH between 8 and 10, the intensity of the free Nd–DOTP resonance increases at the expense of that of the adduct. This can be attributed to the deprotonation of the ammonium groups and the concomitant decrease of the Coulomb interaction between the negatively charged Nd-DOTP species and the CD derivative leading to dissociation of the adduct.

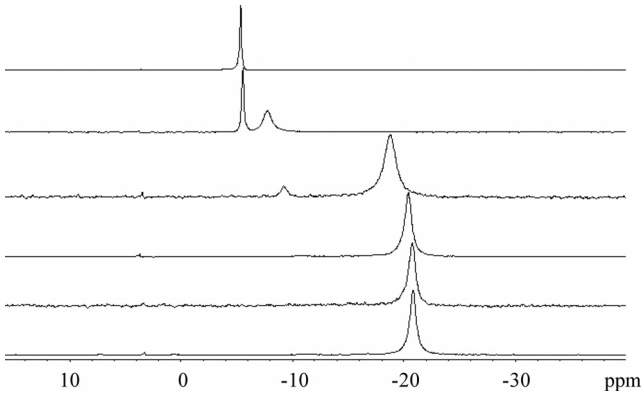

Figure 5. pH dependence of the ^{31}P NMR (202.274 MHz) spectrum of a mixture of γ-CD^+ and Nd–DOTP, in D_2O, $\rho = 1$, 298 K. Bottom to top: pH 5, 6, 7, 8, 9, 10.

Structure Evaluation of the Ln–DOTP-CD^+ Adduct from Lanthanide-Induced Longitudinal Relaxation Rate Enhancements

The solution structure of the 1:1 adduct of Ln–DOTP and the CD^+ was evaluated from the induced ^1H longitudinal relaxation rates. The paramagnetic lanthanide induced shifts for Ln = Gd have no dipolar contribution, but are exclusively from contact origin. Consequently, the Gd^{3+} shifts are relatively small and the exchange of ligands between the free and bound form is usually rapid on the NMR timescale. Longitudinal relaxation rates were determined for the protons of β- and γ-CD^+ in the presence of Gd–DOTP for ρ values up to 0.1 (at pH 7.0) and 0.02 (at pH 9.0) (Figure S3). At pH 7.0 the relaxation rates for all the protons are almost the same and increase linearly with ρ and at pH 9.0 the proton relaxation rates are different, but increase nonlinearly with ρ.

For rapid exchange between free γ-CD^+, Gd–DOTP and their adduct, at low ρ-values, the observed relaxation rates are given by Equation (1).

$$R_{1,obs} = \frac{\rho}{T_{1M} + \tau_M} + R_{1f} \quad (1)$$

Here, $R_{1,obs}$ is the observed longitudinal relaxation rate (the reciprocal of the relaxation time, $1/T_{1obs}$), T_{1M} the longitudinal relaxation time of the proton in question in the adduct, τ_M the residence time in the adduct and R_{1f} the relaxation rate of that proton in the free form. When $\tau_M << T_{1M}$, $R_{1,obs}$ is linearly dependent on ρ and the values of T_{1M} can be determined from the slopes of the lines obtained upon plotting $R_{1,obs}$ as a function of ρ. However, when $\tau_M >> T_{1M}$, the slopes are equal to $1/\tau_M$ for all protons in the adduct. This is apparently the case at pH 7 for Gd–DOTP-CD^+. The nonlinear relationship observed for pH 9 may be explained by a dependence of τ_M on ρ. Under these conditions, an accurate determination of T_{1M} becomes cumbersome and so we decided to select Tm–DOTP for the evaluation of the solution structure of its adduct with the CD^+s. In an ^1H NMR spectroscopic titration with large ρ values ($\rho = 0.25$–5), the exchange of the protons of CD^+s in the adduct and the free form is slow on the ^1H NMR shift timescale: separate sets of signals are observed for both forms (Figure S4). Since the resonances of the

CD^+ protons showed increased broadening and overlap at higher ρ values (Figure S4), we decided to evaluate the paramagnetic relaxation rates of the CD^+ protons induced by Tm–DOTP from the spectra at very low concentration ($\rho = 0.05$). The relaxation rates induced by Tm^{3+} have contributions determined by the dipolar and Curie mechanisms,[2] which are modulated by the electronic relaxation rates and the rotational correlation time, respectively. Since the exchange between the protons of CD^+s in the adduct and the free form is slow on the ^1H NMR timescale in this case, the longitudinal relaxation rates (R_{1M}) can be derived from the observed relaxation rates just by subtraction of the diamagnetic contribution from the observed relaxation rates. The values of R_{1M} obtained for the β- and γ-CD^+ protons at pH 7 and 9 are compiled in Table 1. The proton resonances of the CD^+s were assigned on the basis of the magnitude of the relaxation rate enhancements.

Table 1. R_{1m} values (experimental and theoretical) of the (β,γ)-CD^+ in the presence of the $[Tm(DOTP)]^{5-}$ complex at $\rho = 0.05$, 298 K, pH 7.0 and 9.0.

	per-NH_3^+-β-CD		per-NH_3^+-γ-CD	
	$(R_{1m})_i$ (s^{-1}) Experimental	$(R_{1m})_i$ (s^{-1}) Theoretical	$(R_{1m})_i$ (s^{-1}) Experimental	$(R_{1m})_i$ (s^{-1}) Theoretical
pH 7.0				
H^1	0.12	0.13	0.30	0.26
H^2	0.16	0.18	0.28	0.26
H^3	0.32	0.33	0.20	0.12
H^4	0.26	0.25	0.45	0.44
H^5	0.48	0.49	0.64	0.64
H^{6a}	0.56	0.55	0.78	0.74
H^{6b}	0.43	0.44	0.64	0.64
pH 9.0				
H^1	0.38	0.39	0.40	0.40
H^2	0.32	0.31	0.20	0.19
H^3	0.22	0.23	0.17	0.17
H^4	0.75	0.76	0.77	0.41
H^5	1.15	1.13	1.22	1.21
H^{6a}	4.28	4.31	3.37	3.37
H^{6b}	2.26	2.26	1.84	2.03

The relaxation rates R_{1M} have contributions from the dipolar and the Curie relaxation mechanisms. It can be deduced that they are related to the structure of the paramagnetic systems involved by Equation (2).[3]

$$R_{1M} = k/r^6 \quad (2)$$

Here, r is the distance between the Tm^{3+} ion in the system and the CD^+ proton in question.

The molecular structure of the Tm–DOTP part of the 1:1 adduct with the CD^+s was assumed to be identical to the crystal structure of Tm–DOTP[38] and molecular models of the CD^+ moieties were constructed by attaching ammonium substituents to the upper rim of the crystal structures of the parent CDs,[40] followed by optimisation of the geometries of the $–CH_2–NH_3^+$ functions using molecular mechanics with the MM+ force field. The Tm–DOTP chelate was located at the top of the per-aminated rim of the CD^+, with the Tm^{3+} ion and the centre of the DOTP macrocyclic ring on the Z axis of the coordinate system whose origin corresponds to the centre of the cyclodextrin skeleton. The experimental R_{1M} data were fitted to Equation (2) by varying the distance between the Tm^{3+} ion and the centre of the CD^+, which was taken as the origin of the coordinate system. For the data measured at pH 7.0, good fits were obtained for a distance of 10.79 and 10.45 Å for β- and γ-CD^+, respectively, whereas the best-fit values of these distances for the data measured at pH 9.0 were significantly shorter, 9.22 and 8.88 Å, respectively. The relaxation rates calculated with these best-fit distances are compared with the experimental values in Table 1.

The decrease of the best-fit distance upon increase of the pH from 7 to 9 is in agreement with the increasing charge of the Tm–DOTP species due to its deprotonation and underlines the importance of the electrostatic interaction between the positively charged protonated amino groups of the CDs and the negatively charged phosphonate oxygens of the Ln–DOTP complex for the stabilization of the supramolecular adduct.

Molecular models (Figure 6) show that the structures of the adducts allow for the formation of hydrogen bonds between the amine NH protons of the host and the phosphonate oxygens of the guest. Surprisingly, the Tm–DOTP complex is located outside the β-cavity, even for γ-CD^+. Entering the cavity would require the Tm–DOTP complex to approach the upper rim of the CD^+ with the DOTP functions directed away from the ammonium functions and the hydrophobic macrocyclic entity towards them, which apparently is much less favourable than an approach with the opposite orientation of Tm–DOTP, and hence this does not occur.

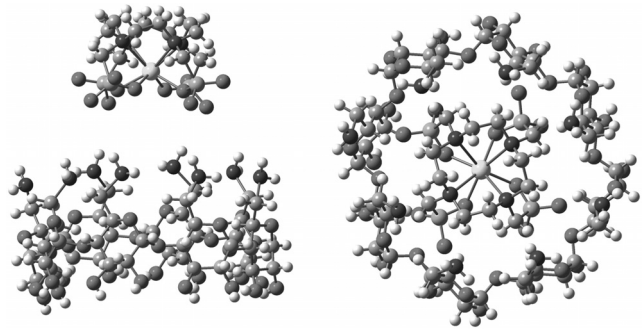

Figure 6. Model of the interaction between Tm–DOTP and γ-CD^+, side view (left) and top view (right). The value calculated for the distance between the lanthanide ion and the origin of the coordinate system (at the centre of the γ-CD^+) was 8.88 Å, at pH 9.0.

^1H Longitudinal Relaxivity Studies

The pH effects on the stability of the Gd–DOTP-CD^+ adducts were also studied through investigation of the water ^1H longitudinal relaxation rates in the presence of this system. In a first step, a 1 mM solution of Gd–DOTP was titrated with increasing amounts of the neutral β-CD or γ-CD up to a value of $\rho = 5.0$, at 9 MHz, pH 7 and 298 K.

This had no effect on the relaxivity, which did not change from the values for Gd–DOTP alone (r_1 = 5.1 ± 0.3 s^{-1} mM^{-1}), indicating that the interactions with the parent CDs are absent or too weak to change r_1.[24,25]

By contrast, the interaction of Gd–DOTP with the charged β- and γ-CD^+ (see Figure 7) gives rise to a gradual increase in r_1 with the pH up to a maximum of pH ≈ 9, and then drops steeply to the value for free Gd–DOTP at pH 10. This reflects the pH dependence of the supramolecular interaction, which is determined by the protonation state and the charge of the negatively charged guest chelate and the positively charged host cyclodextrin, as reflected in their pK_a values, as discussed before.

Relaxometric titrations were then carried out for Gd–DOTP solutions containing increasing concentrations of β- or γ-CD^+, up to ρ = 5, both at pH 7.0 and at pH 9.0, a value close to the pH of maximum interaction (Figure 8). For the β-CD^+/Gd–DOTP system, the shape of the titration curves again shows that the maximum relaxivity obtained and the association constants are much higher at pH 9 than at pH 7. The titration curve at pH 7 was fitted to the formation of a single 1:1 supramolecular species, with a calculated conditional association constant K_A = $(1.19 \pm 0.47) \times 10^4$ M^{-1}. The K_A value at pH 9.0 is at least an order of magnitude higher, which is too high to be determined from the experimental data. This once again reflects stronger electrostatic interactions at pH 9, resulting from the larger negative charge of the Gd^{3+} complex (–5), while the β-CD^+ is still partially protonated. For the γ-CD^+/Gd–DOTP system, the titration curve obtained at pH 7 is more complex, with a marked relaxivity decrease at higher γ-CD^+ concentrations. This indicates that the adduct formation may involve M_2L species, whose lower relaxivity might be explained by a weaker interaction of the second Gd–DOTP species with the opposite rim of the γ-CD^+, thus partially hindering the access of the outer-sphere molecules to the proximity of the Gd^{3+} ions. At pH 9 it has the typical shape of a 1:1 binding isotherm, with a calculated conditional as-

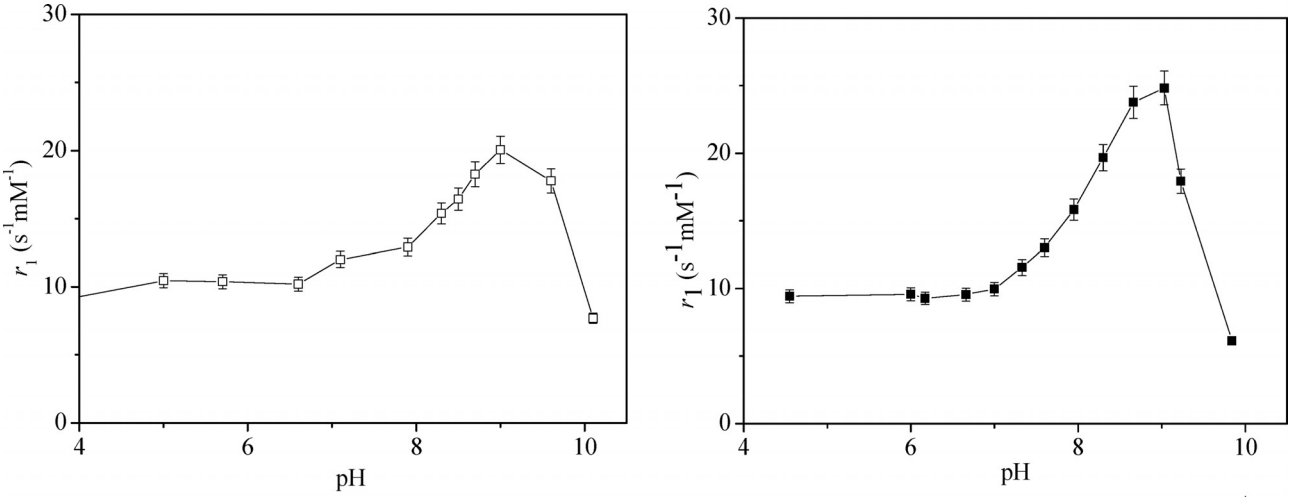

Figure 7. pH dependence of r_1 for solutions containing 1 mM Gd–DOTP and 5 mM β-CD^+ (left) or γ-CD^+ (right) at 9 MHz, 298 K.

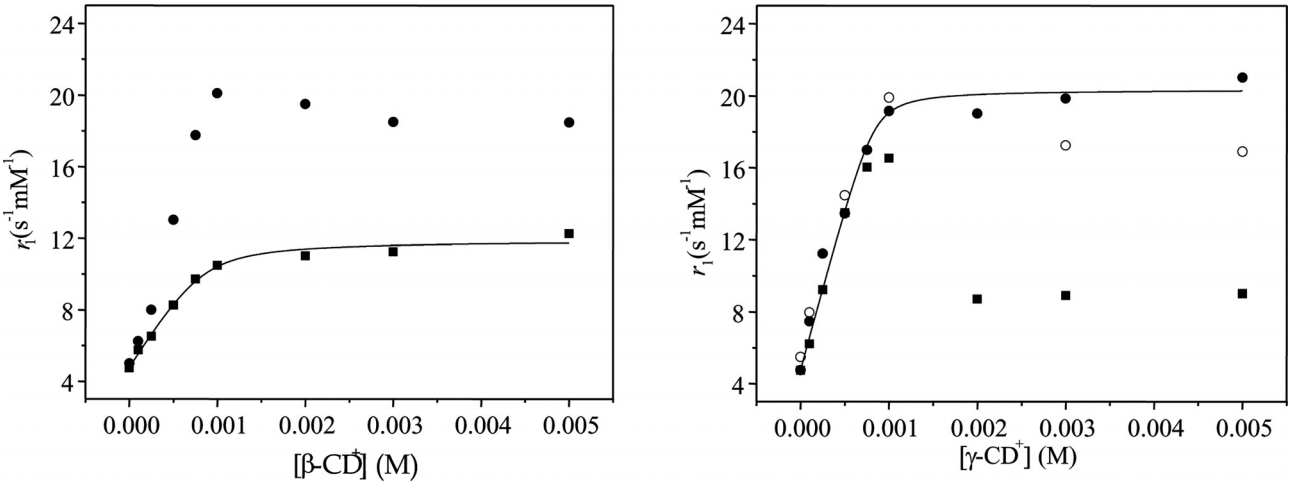

Figure 8. $[Gd(DOTP)]^{5-}$ relaxivities as a function of CD^+ concentration, 9 MHz and 298 K; $[Gd(DOTP)]^{5-}$ concentration is 1 mM. Left: β-CD^+ at pH 7 (●) and pH 9 (■). Right: γ-CD^+ at pH 7 (■), pH 8 (○) and pH 9 (●). The lines through some of the data correspond to the best-fit parameters described in the text.

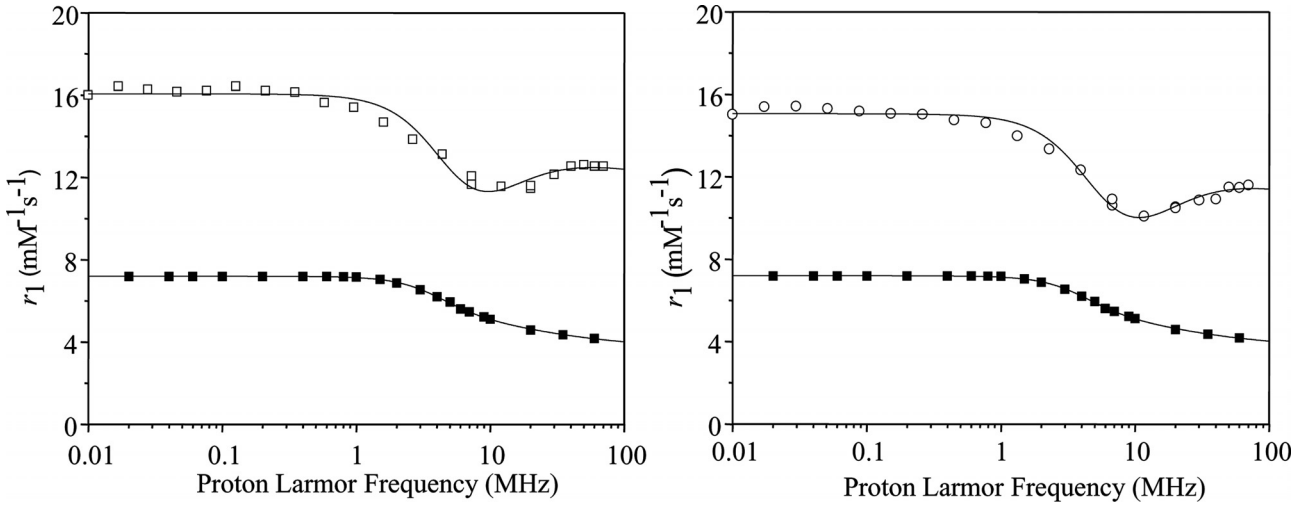

Figure 9. ^{1}H NMRD profiles of Gd–DOTP in the absence (■) and presence of β-CD$^+$ (□, ρ = 1) and γ-CD$^+$ (○,ρ = 0.5) (pH 7.4, 298 K). The lines through some of the data correspond to the best-fit parameters described in the text.

Table 2. Parameters obtained from the NMRD data of (β,γ)-CD$^+$/[Gd(DOTP)]$^{5-}$.

	[Gd(DOTP)]$^{5-}$	β-CD$^+$/[Gd(DOTP)]$^{5-}$ (1:1)	γ-CD$^+$/[Gd(DOTP)]$^{5-}$ (1:0.5)
$\Delta^2/10^{19}$ [s^{-2}]	2.36	4.00	5.27
τ_V^{298} [ps]	32.70	24.80	19.68
q	0	0	0
$a_{GdH}/10^{-10}$ [m]	3.8	3.8	3.8
$D/10^{-9}$ [m^2 s^{-1}]	2	2	2
q'	4	15.71	15.65
$r_{(sf)}/10^{-10}$ [m]	4.33	4.33	4.33
$\tau_{c(sf)}/10^{-10}$ [s]	1.23	1.57	1.45

sociation constant $K_A = (4.80 \pm 0.50) \times 10^4$ м$^{-1}$, slightly higher than for the β-CD$^+$.

As Gd–DOTP has no inner-sphere water molecules (q = 0), the ^{1}H NMRD profiles obtained for β- and γ-CD$^+$/Gd–DOTP at pH 7.4 (Figure 9) were fitted by using a combination of the second-sphere[41a] and the outer-sphere[41b] relaxation models. The magnetic field dependency of the inner-sphere relaxivity of small Gd^{3+} complexes is usually described by the Solomon–Bloembergen–Morgan (SBM) equations, despite its many approximations.[42] Although more realistic theoretical alternatives to the description of electronic spin relaxation, in particular for large, slow tumbling systems do exist,[43] the SBM theory is used here as a simple way to account for the effects of electronic spin relaxation on relaxivity, yielding only "ad hoc" ZFS parameter values. The SBM equations can be adapted to second-sphere effects,[41a] while Freed's equation is used to describe the outer-sphere contribution of the relaxivity.[41b] The set of equations used is given in the Supporting Information. Second-sphere relaxivity depends on a variety of parameters, such as the average number of second-sphere water molecules (q'), the average distance of their protons from the Gd^{3+} ion ($r_{(sf)}$, where the subscript refers to second-sphere), the correlation time responsible for the second-sphere contribution ($\tau_{c(sf)}$) [which is the combination between the residence lifetime of the second-sphere water protons ($\tau_{M(sf)}$) and their reorientational correlation time ($\tau_{r(sf)}$)] and the electronic relaxation parameters (the static zero-field splitting, Δ^2, and the correlation time for its modulation, τ_v). The outer-sphere contribution depends on the distance of closest approach of a water molecule to Gd^{3+} (a_{GdH}), the diffusion constant (D) and the electronic relaxation time at zero field (τ_{S0}), which is a function of Δ^2.

The best-fit parameters, obtained upon keeping the parameters a_{GdH}, D and $r_{(sf)}$ constant at the values obtained for Gd–DOTP, are presented in Table 2. Here, it seems that the relaxivity enhancement of Gd–DOTP upon interaction with β- or γ-CD$^+$ arises from the increase of the average number of second-sphere water protons (q'), whereas the correlation time responsible for the second-sphere contribution ($\tau_{c(sf)}$) is practically unaltered.

PARACEST Studies

We also investigated the paramagnetic CEST (PARACEST)[35] properties of the supramolecular adducts formed between the positively charged (β,γ)-CD$^+$s, which contain a relatively high number of exchanging protons (21 and 24 mobile protons for β- and γ-CD$^+$, respectively) and the negatively charged complex Tm–DOTP. It is expected that the paramagnetic complex may act as a shift reagent for the resonances of the amine protons of the cationic cyclodextrins in order to make them detectable in a CEST

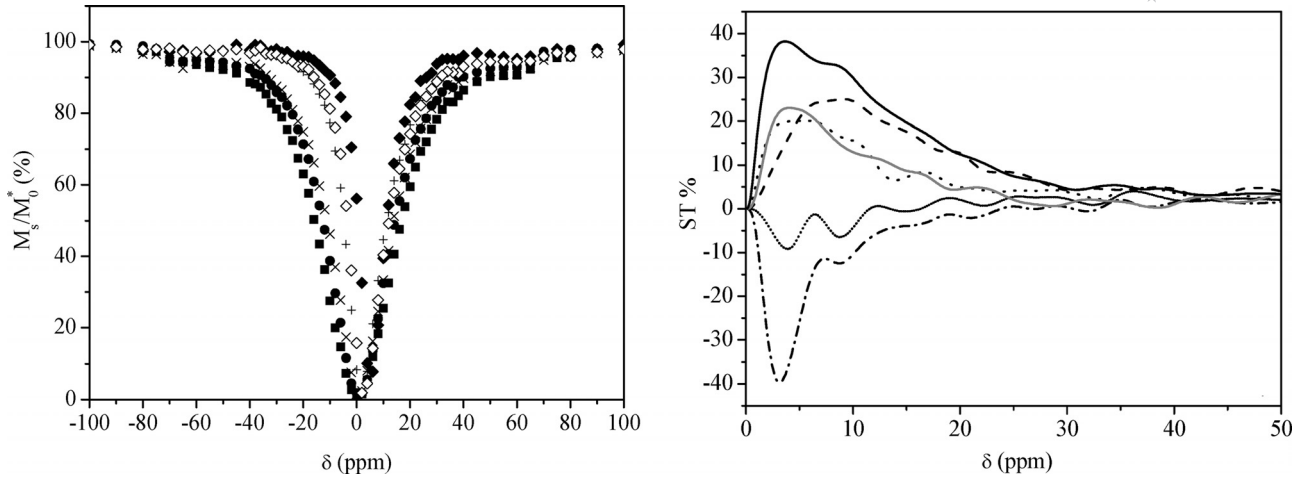

Figure 10. CEST Z-spectra (left) and ST-profiles (right) of an aqueous solution of 5 mM β-CD^+ in the presence of Tm–DOTP at different molar ratios (7.05 T, pH 7.4, 298 K). Irradiation conditions: block pulse, irradiation time 2 s, B_1 intensity 12 μT. The CEST spectra correspond to Tm–DOTP to β-CD^+ ratios of 10:1 (■), 5:1 (●), 4:1 (×), 2:1 (+), 1:1 (◇) and 0.5:1 (♦). The corresponding ST/profiles correspond to the same ratios 10:1 (dash dot), 5:1 (short dot), 4:1 (dot), 2:1 (dash), 1:1 (solid) and 0.5:1 (light solid). ST% is defined as $100 \times (1 - M_s/M_0)$.

experiment, as it has been observed for the guanidine protons of polyarginine in the presence of Tm–DOTP.[44]

Figure 10 shows the Z- and the ST-spectra of solutions containing different Tm–DOTP/β-CD^+ molar ratios (ρ = 0.5 to 10), with the concentration of β- or γ-CD^+ fixed at 5 mM, leading to the presence in solution of more than 100 mM of mobile protons. The main feature of the Z-spectra is the broadening of the CEST peak of the bulk water upon increasing the concentration of the paramagnetic agent. The corresponding ST profiles reported in Figure 10 (right) do not show any clear ST effect arising from mobile protons shifted by the paramagnetic agent. The only peak detectable in the ST profiles falls very close to the bulk water signal (within 5 ppm), and, furthermore, its offset sign displays an unusual dependence on the ρ values (shift positive for $\rho < 5$, and negative for $\rho > 5$) (see Figure S5).

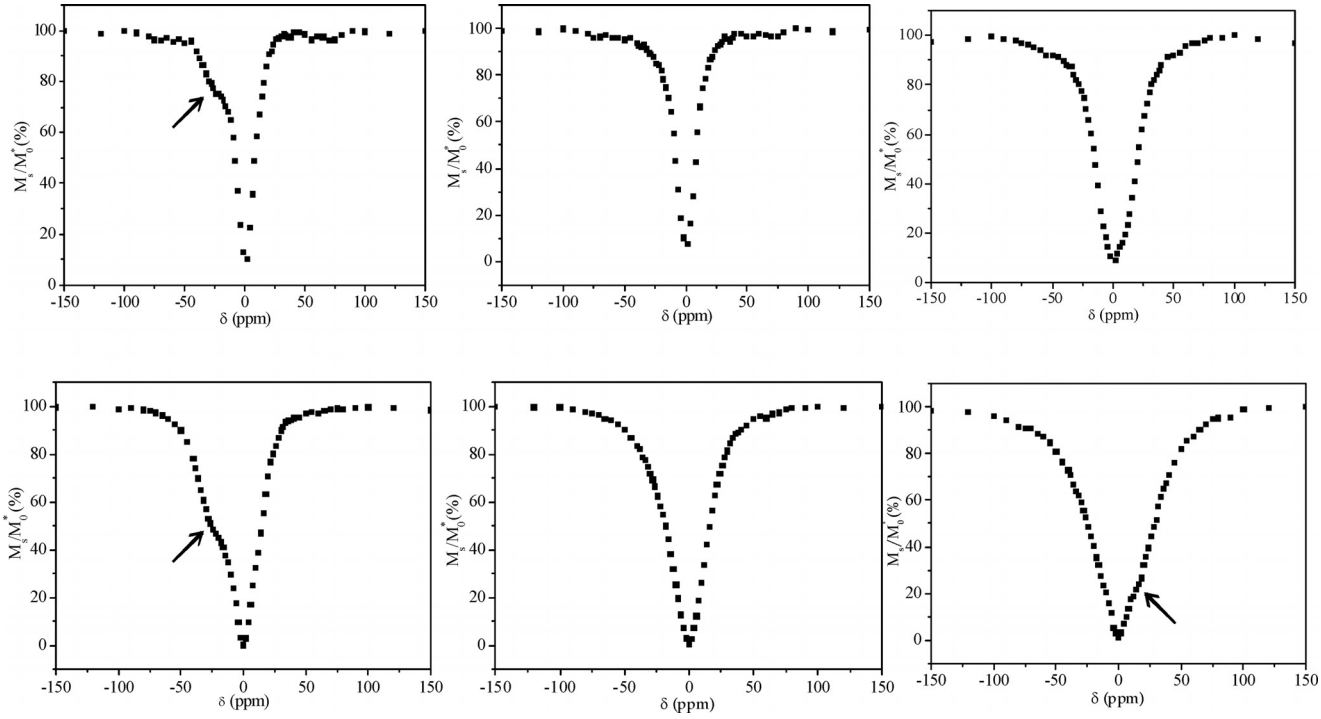

Figure 11. CEST spectra of γ-CD^+ aqueous solution (7.05 T, 5 mM, pH 7.4, 298 K) in the presence of Tm–DOTP at different molar ratios (left ρ = 0.5, middle ρ = 0.6 and right ρ = 0.7), measured at two different saturation intensities: 12 μT (top) and 24 μT (bottom). Irradiation conditions: block pulse, irradiation time 2 s.

The CEST experiments carried out with the γ-CD^+ in the presence of the Tm–DOTP complex showed similar results. Surprisingly, and differently from β-CD^+, only solutions with Tm–DOTP/γ-CD^+ molar ratios lower than 1 could be analyzed, because at higher molar ratios a precipitation occurred. Figure 11 shows the Z-spectra for the investigated molar ratios measured at two different B_1 intensities (12 and 24 μT, top and bottom, respectively). The Z-spectra at the molar ratio $\rho = 0.5$ are characterized by the presence of a shoulder of the CEST peak of the bulk water at about –30 ppm, which is analogous to the shift reported for the guanidine protons of polyarginine in the presence of the same paramagnetic shift reagent.[44] Surprisingly, upon increasing the amount of γ-CD^+, the shoulder disappears at $\rho = 0.6$ and reappears at the opposite side (ca. 20 ppm) at $\rho = 0.7$. This behaviour is more evident by looking at the ST profiles reported in Figure S6 for the experiments carried out at 24 μT.

This finding is similar to what was observed for the adduct with β-CD^+ (see the right side of Figure 10) even if in that case the frequency offset of the detected CEST peak was very small (less than 5 ppm). The similarity between the behaviour of the two supramolecular adducts suggests that the CEST peak detected for the β-CD^+ adduct might be assigned to the amine protons of the cyclodextrin, which are the only mobile protons present in these systems. On this basis, the different induced shift between β-CD^+ and γ-CD^+ could be the result of a different interaction modality between the two different CD^+s and the shift reagent. A possible way to investigate these changes more intensely could be the cocrystallization of the lanthanide complex and the charged CD^+s.

The large changes of the ST profiles observed upon very small changes in the molar ratio of the two interacting molecules is an indication of the complexity of this noncovalent interaction, which likely involves the formation of adducts with different stoichiometries.

Conclusions

The data presented in this work shows that the positively charged β- and γ-CD^+ form strong 1:1 and weaker 1:2 adducts with negatively charged Ln-DOTP complexes. The main driving force is an electrostatic interaction between the oppositely charged complexes, which is nicely illustrated by the increasing stability upon increase of the pH. Surprisingly, the Ln–DOTP complexes were not included in the cavity of these charged cyclodextrins. In a previous investigation, it was shown that Ln–DOTA complexes partly enter the cavity of neutral γ-CD; the carboxylate groups remain outside the cavity.[25] The reluctance of β- and γ-CD^+ to form inclusion compounds with Ln–DOTP can be rationalized by steric hindrance on entering the cavity due to the substituents at the upper rim of the cyclodextrin and to the high hydrophylicity of Ln–DOTP, which results in a lower affinity than Ln–DOTA for the hydrophobic cavity of cyclodextrins.

The two enantiomeric forms of the TSAP isomer of Nd–DOTP could in principle be distinguished by NMR spectroscopy through the binding of an optically active substrate such as β- or γ-CD^+. However, such a chiral resolution of the two enantiomeric forms was not observed, as opposed to the previously studied system formed by ion-pairing of Eu–DOTP with the optically active organic base meglumine [*N*-methyl-D(–)-glucamine].[44b] This difference in behaviour of the two systems probably reflects the relatively large distance between the amine NH protons of the host CD^+ and the phosphonate oxygens of the guest Ln–DOTP in the presently studied adducts. The interaction between Ln–DOTP and β- or γ-CD^+ is reinforced through formation of hydrogen bonds. This also considerably increases the number of second-sphere water molecules trapped in their interface, which leads to a substantial relaxivity enhancement for the Gd–DOTP complex upon adduct formation.[38] This interaction is also responsible for the observed shift of the saturation transfer peaks of the ammonium functions of the positively charged CDs caused by the Tm–DOTP complex, in particular for the γ-CD derivative.

Modified charged cyclodextrins have been used before as scaffolds for the covalent attachment of stable macrocyclic Gd^{3+} complexes or of Gd^{3+} ions forming weaker complexes.[15] They have been applied as MRI contrast agents for cell imaging[15d] and evaluated in an in vivo tumour animal model.[45] However, the present work indicates that the formation of stable adducts combining the CD properties with the stability of macrocyclic Gd^{3+} chelates could be a useful alternative to the in vivo use of poorly stable Gd^{3+}-CD complexes.

Experimental Section

Syntheses, Chemicals and Sample Preparations: The synthesis of per-NH_3^+-(β,γ)-CD (β,γ-CD^+) was carried out following the procedure described previously.[46]

β-CD^+: ^{1}H NMR (D_2O, TSP, pH 6.9, 300 MHz): $\delta = 5.15$ (d, 7 H, H1); $\delta = 4.16$ (t, 7 H, H5); $\delta = 3.96$ (dd, 7 H, H3); $\delta = 3.63$ (dd, 7 H, H2); $\delta = 3.55$ (dd, 7 H, H4); $\delta = 3.42$ (dd, 7 H, $H6_a$); $\delta = 3.26$ (dd, 7 H, $H6_b$) ppm. ^{13}C NMR (D_2O, *t*BuOH, pH 6.9): $\delta = 103.31$ (C1); $\delta = 84.50$ (C4); $\delta = 74.42$ (C2); $\delta = 73.25$ (C3); $\delta = 72.03$ (C5); $\delta = 52.54$ (C6) ppm.

γ-CD^+: ^{1}H NMR (D_2O, TSP, pH 7.1, 300 MHz): $\delta = 5.18$ (d, 8 H, H1); $\delta = 4.14$ (t, 8 H, H5); $\delta = 3.98$ (dd, 8 H, H3); $\delta = 3.69$ (dd, 8 H, H2); $\delta = 3.60$ (dd, 8 H, H4); $\delta = 3.42$ (dd, 8 H, $H6_a$); $\delta = 3.23$ (dd, 8 H, $H6_b$) ppm. ^{13}C NMR (D_2O, *t*BuOH, pH 7.1): $\delta = 103.95$ (C1); $\delta = 84.64$ (C4); $\delta = 74.62$ (C2); $\delta = 73.29$ (C3); $\delta = 72.12$ (C5); $\delta = 52.71$ (C6) ppm.

The macrocyclic ligand H_8DOTP was synthesized according to a known procedure,[47] or purchased from Macrocyclics, Dallas, Texas, USA (H_8DOTP). The $LnCl_3$ salts were purchased from Aldrich. The deuterated solvents D_2O (99.9 atom-% D), DCl (99.9 atom-% D) and NaOD (99.9 atom-% D, 40% solution in D_2O) were obtained from Sigma. The Ln–DOTP complexes were prepared following the procedures described in the literature.[39] The final solutions were tested for the absence of free lanthanide ions using xylenol orange as indicator.[48]

The NMR titrations were performed by adding an aqueous solution containing the cyclodextrin (5 mM) and the chelate (1 mM) to an aqueous solution (1 mM) of the lanthanide chelate. A solution of TSP [sodium 3-(trimethylsylyl)propionate] in $CDCl_3$ in a coaxial tube inside the NMR sample tube was used as external reference for proton shifts in order to prevent the interaction between the CDs and the standard. ^{31}P NMR shifts were referenced to 85% H_3PO_4 as external standard.

pD measurements were carried out with a Crison micropH 2000 pH meter, coupled to a SemTix Mic pH 014/0 electrode. The pD values were adjusted with DCl or NaOD and the pH meter readings were converted to pD values using the isotopic correction (pD = pH reading + 0.4).[49]

Spectrometric Measurements: Electrospray mass spectra were obtained with a Q-tof 2 mass spectrometer (Micromass, Manchester, UK). The source was operated in the positive ion mode at a capillary voltage of 3 kV. NaI was used for the calibration. Samples dissolved in water were injected at a flow rate of a 5 $\mu L\,min^{-1}$.

^1H NMR spectra were obtained with Varian Unity INOVA 300 (300.154 MHz), VXR-400S (399.918 MHz) or Unity 500 (499.824 MHz) spectrometers. ^{13}C NMR spectra were measured with the INOVA 300 or the VXR-400S (75.481 and 100.569 MHz, respectively) spectrometers and ^{31}P NMR spectra on the UNITY 500 (202.274 MHz) spectrometer. The probe temperature was adjusted with a precision of ±0.5 °C. Spin-lattice relaxation rates for the supramolecular systems were measured using the inversion recovery method and were corrected for the diamagnetic contribution by subtracting 1.2 s^{-1}, which is the average longitudinal relaxation rate of the CD^+ protons in the free form. Transverse relaxation rates were evaluated from the linewidths, which were corrected for the diamagnetic contribution by the subtraction of 18.8 Hz, the average linewidth for the various free CD^+ protons. All the chemical exchange saturation transfer (CEST) experiments were carried out with a Bruker Avance 300 spectrometer equipped with a microimaging probe. The solutions for the CEST experiments were prepared in distilled water and the pH was kept at 7.4 by the addition of a buffer (HEPES, 1 mM) without salts, while all other NMR spectroscopic experiments were performed with D_2O solutions without HEPES.

Relaxometric measurements were carried out at 9 MHz and 25 °C with a MS4 relaxometer (Joseph Stephan Institute, Ljubljana, Slovenia). The NMRD profiles were measured using a Stelar Spinmaster FFC NMR relaxometer (0.01–40 MHz), equipped with a VTC-91 temperature control unit and the temperature was controlled by gas flow. The data points collected at higher frequency were obtained using an electromagnet with tunable coils in the range of 20 to 80 MHz.

Computer Calculations: Molecular Mechanics were performed using the HyperChem program (version 7.5, MM+ force field, HyperCube Inc., Gainsville, FI). The three-dimensional structures obtained were represented using the program GaussView[50]. The computer fittings of the $1/T_1$ data were performed with the program Micromath Scientist[51] and those of the NMRD data with OriginPro.[52]

Supporting Information (see footnote on the first page of this article): Mass spectrum of γ-CD^+/Gd–DOTP, ρ = 1, pH 9.0 and pH 7.0; (a) ^1H NMR titration (500 MHz) of γ-CD^+ with Nd–DOTP in D_2O, pH 7.0, 298 K. Expansion of the diamagnetic region of the spectra. Proton relaxation rate enhancements for 5 mM β- and for γ-CD^+ induced in the presence of increasing concentrations of Gd–DOTP, at pH 7.0 and 9.0, D_2O solution (500 MHz, 298 K). ^1H NMR titration (500 MHz) in D_2O of β-CD^+ (5 mM) with Tm–DOTP (pH 7.3, 298 K). Expansion of the spectra in (a) in the 8 to 40 ppm region. Expansion of the diamagnetic region of the spectra. ST effects (at 3.8 ppm) of β-CD^+ in the presence of Tm–DOTP as a function of their molar ratio (H_2O, 5 mM, pH 7.4, 7.05 T, 298 K). A negative ST effect means that a CEST contrast is detected at offset frequencies with opposite sign (here –3.8 ppm). ST profiles of γ-CD^+ in the presence of Tm–DOTP at different molar ratios (7.05 T, 5 mM, pH 7.4, 298 K). Irradiation conditions: block pulse, irradiation time 2 s, B_1 intensity 24 μT.

Acknowledgments

This work was supported by the Fundação para a Ciência e a Tecnologia (FCT), with coparticipation of the European Community funds FEDER, for the financial support under project PTDC/QUI/70063/2006 (grant number SFRH/BPD/35005/2007; to G. A. P.) The Varian VNMRS 600 NMR spectrometer used in Coimbra is part of the National NMR Network and was purchased in the framework of the National Program for Scientific Re-equipment, contract REDE/1517/RMN/2005, with funds from POCI 2010 (FEDER) and FCT. This project was carried out within the framework of the COST Action D38 "Metal-Based Systems for Molecular Imaging Applications".

[1] P. Caravan, J. J. Ellison, T. J. McMurry, R. B. Lauffer, *Chem. Rev.* **1999**, *99*, 2293–2352.
[2] V. Jacques, J. F. Desreux, *Top. Curr. Chem.* **2002**, *221*, 123–164.
[3] J. A. Peters, J. Huskens, D. J. Raber, *Prog. Nucl. Magn. Reson. Spectrosc.* **1996**, *28*, 283–350.
[4] S. Aime, M. Botta, M. Fasano, E. Terreno, *Chem. Soc. Rev.* **1998**, *27*, 19–29.
[5] É. Tóth, L. Helm, A. E. Merbach, *Top. Curr. Chem.* **2002**, *221*, 61–101.
[6] a) É. Tóth, L. Helm, K. E. Kellar, A. E. Merbach, *Chem. Eur. J.* **1999**, *5*, 1202–1211; b) F. A. Dunand, É. Tóth, R. Hollister, A. E. Merbach, *J. Biol. Inorg. Chem.* **2001**, *6*, 247–255; c) M. G. Duarte, M. H. Gil, J. A. Peters, J. M. Colet, L. Vander Elst, R. N. Muller, C. F. G. C. Geraldes, *Bioconjugate Chem.* **2001**, *12*, 170–177.
[7] a) D. M. Corsi, L. Vander Elst, R. N. Muller, H. van Bekkum, J. A. Peters, *Chem. Eur. J.* **2001**, *7*, 64–71; b) J. P. André, C. F. G. C. Geraldes, J. A. Martins, A. E. Merbach, M. I. M. Prata, A. C. Santos, J. J. P. de Lima, É. Tóth, *Chem. Eur. J.* **2004**, *10*, 5804–5816; c) P. Baía, J. P. André, C. F. G. C. Geraldes, J. A. Martins, A. E. Merbach, É. Tóth, *Eur. J. Inorg. Chem.* **2005**, 2110–2119.
[8] a) Protein-Bound Metal Chelates: S. Aime, M. Fasano, E. Terreno, M. Botta, in: *The Chemistry of Contrast Agents in Medical Magnetic Resonance Imaging* (Eds.: É. Tóth, A. E. Merbach), Wiley, Chichester, **2001**, p. 193; b) S. Aime, M. Botta, S. G. Crich, G. Giovenzana, G. Palmisano, M. Sisti, *Bioconjugate Chem.* **1999**, *10*, 192–199; c) S. Aime, M. Botta, M. Fasano, S. G. Crich, E. Terreno, *J. Biol. Inorg. Chem.* **1996**, *1*, 312–319.
[9] a) É. Tóth, D. Pubanz, S. Vauthey, L. Helm, A. E. Merbach, *Chem. Eur. J.* **1996**, *2*, 1607–1615; b) L. H. Bryant Jr, M. W. Brechbiel, C. Wu, J. W. M. Bulte, V. Herynek, J. A. Frank, *J. Magn. Reson. Imaging* **1999**, *9*, 348–352; c) G. M. Nicolle, É. Tóth, H. Schmitt-Willich, B. Radüchel, A. E. Merbach, *Chem. Eur. J.* **2002**, *8*, 1040–1048; d) S. Laus, A. Sour, R. Ruloff, É. Tóth, A. E. Merbach, *Chem. Eur. J.* **2005**, *11*, 3064–3076.
[10] a) S. Aime, M. Botta, M. Fasano, S. G. Crich, E. Terreno, *J. Biol. Inorg. Chem.* **1996**, *1*, 312–319; b) S. Aime, M. Botta, S. G. Crich, G. B. Giovenzana, R. Pagliarin, M. Piccinini, M. Sisti, E. Terreno, *J. Biol. Inorg. Chem.* **1997**, *2*, 470–479; c) S. Aime, M. Botta, L. Frullano, S. G. Crich, G. B. Giovenzana, R. Pagliarin, G. Palmisano, M. Sisti, *Chem. Eur. J.* **1999**, *5*, 1253–1260;

d) P. Caravan, N. J. Cloutier, M. T. Greenfield, S. A. McDermid, S. U. Dunham, J. W. M. Bulte, J. C. Amedio Jr, R. J. Looby, R. M. Supkowski, W. DeWitt Horrocks Jr, T. J. McMurry, *J. Am. Chem. Soc.* **2002**, *124*, 3152–3162.
[11] D. Thonon, V. Jacques, J. F. Desreux, *Contrast Media Mol. Imaging* **2007**, *2*, 24–34.
[12] a) J. P. André, É. Tóth, H. Fisher, A. Seelig, H. R. Mäcke, A. E. Merbach, *Chem. Eur. J.* **1999**, *5*, 2977–2983; b) G. M. Nicolle, É. Tóth, K. P. Eisenwiener, H. R. Mäcke, A. E. Merbach, *J. Biol. Inorg. Chem.* **2002**, *7*, 757–769; c) K. Kimpe, T. N. Parac-Vogt, S. Laurent, C. Piérart, L. Vander Elst, R. N. Muller, K. Binnemans, *Eur. J. Inorg. Chem.* **2003**, *16*, 3021–3027.
[13] a) S. L. Fossheim, A. K. Fahlvik, J. Klaveness, R. N. Muller, *Magn. Reson. Imaging* **1999**, *17*, 83–89; b) V. Weissig, J. Babich, V. Torchilin, *Colloids Surf. B* **2000**, *18*, 293–299; c) C. Gløgård, G. Stensrud, R. Hovland, S. L. Fossheim, J. Klaveness, *Int. J. Pharm.* **2002**, *233*, 131–140; d) K.-E. Løkling, S. L. Fossheim, J. Klaveness, R. Skurtveit, *J. Controlled Release* **2004**, *98*, 87–95.
[14] a) S. Morel, E. Terreno, E. Ugazio, S. Aime, M. R. Gasco, *Eur. J. Pharmaceutics Biopharmaceutics* **1998**, *45*, 157–163; b) C. Gløgård, G. Stensrud, J. Klaveness, *Int. J. Pharm.* **2003**, *253*, 39–48.
[15] a) S. D. Kean, C. J. Easton, S. F. Lincoln, *Aust. J. Chem.* **2001**, *54*, 535–539; b) P. J. Skinner, A. Beeby, R. S. Dickins, D. Parker, S. Aime, M. Botta, *J. Chem. Soc. Perkin Trans. 2* **2000**, 1329–1338; c) C. S. Bonnet, P. H. Fries, A. Gadelle, S. Gambarelli, P. Delangle, *J. Am. Chem. Soc.* **2008**, *130*, 10401–10413; d) Z. Kotkova, J. Kotek, D. Jirék, P. Jendelov, V. Herynek, Z. Berkov, P. Hermann, I. Lukeš, *Chem. Eur. J.* **2010**, *16*, 10094–10102.
[16] F. Guillo, B. Amelin, L. Jullien, J. Canceill, J.-M. Lehn, L. D. Robertis, H. Rodriguez, *Bull. Soc. Chim. Fr.* **1995**, *132*, 857–866.
[17] W. Saenger, *Angew. Chem.* **1980**, *92*, 343; *Angew. Chem. Int. Ed. Engl.* **1980**, *19*, 344–362.
[18] T. Loftsson, D. Duchene, *Int. J. Pharm.* **2007**, *329*, 1–11.
[19] C. Jaime, J. Redondo, F. Sanchez-Ferrando, A. Virgili, *J. Org. Chem.* **1990**, *55*, 4772–4776.
[20] M. V. Rekharsky, H. Yamamura, M. Kawai, Y. Inoue, *J. Org. Chem.* **2003**, *68*, 5228–5235.
[21] F. Vögtle, W. M. Müller, *Angew. Chem.* **1979**, *91*, 676; *Angew. Chem. Int. Ed. Engl.* **1979**, *18*, 623–624.
[22] S. Kamitori, K. Hirotsu, T. Higuchi, *J. Chem. Soc. Commun.* **1986**, 690–691.
[23] S. Kamitori, K. Hirotsu, T. Higuchi, *J. Am. Chem. Soc.* **1987**, *109*, 2409–2414.
[24] A. D. Sherry, R. Zarzycki, C. F. G. C. Geraldes, *Magn. Reson. Chem.* **1994**, *32*, 361–365.
[25] E. Zitha-Bovens, H. van Bekkum, J. A. Peters, C. F. G. C. Geraldes, *Eur. J. Inorg. Chem.* **1999**, 287–293.
[26] E. Henriques, M. Bastos, C. F. G. C. Geraldes, M. J. Ramos, *Int. J. Quantum Chem.* **1999**, *73*, 237–248.
[27] a) S. Aime, M. Botta, M. Panero, M. Grandi, F. Uggeri, *Magn. Reson. Chem.* **1991**, *29*, 923–927; b) S. Aime, E. Gianolio, E. Terreno, I. Menegotto, C. Bracco, L. Milone, G. Cravotto, *Magn. Reson. Chem.* **2003**, *41*, 800–805.
[28] S. Aime, E. Gianolio, E. Terreno, G. B. Giovenzana, R. Pagliarin, M. Sisti, G. Palmisano, M. Botta, M. P. Lowe, D. Parker, *J. Biol. Inorg. Chem.* **2000**, *5*, 488–497.
[29] a) S. Aime, M. Botta, F. Fedeli, E. Gianolio, E. Terreno, P. Anelli, *Chem. Eur. J.* **2001**, *7*, 5261–5269; b) E. Battistini, E. Gianolio, R. Gref, P. Couvreur, S. Fuzerova, M. Othman, S. Aime, B. Badet, P. Durand, *Chem. Eur. J.* **2008**, *14*, 4551–4561.
[30] T. Kitae, T. Nakayama, K. Kano, *J. Chem. Soc. Perkin Trans. 2* **1998**, 207–212.
[31] K. Kano, T. Kitae, H. Takashima, Y. Shimofuri, *Chem. Lett.* **1997**, *26*, 899–900.
[32] K. X. Wan, M. L. Gross, T. Shibue, *J. Am. Soc. Mass Spectrom.* **2000**, *11*, 450–457.
[33] M. Guo, S. Zhang, F. Song, D. Wang, Z. Liu, S. Liu, *J. Mass Spectrom.* **2003**, *38*, 723–731.
[34] V. Henrotte, S. Laurent, V. Gabelica, L. Vander Elst, E. Depauw, R. N. Muller, *Rapid Commun. Mass Spectrom.* **2004**, *18*, 1919–1924.
[35] S. Zhang, M. Merritt, D. E. Woessner, R. E. Lenkinski, A. D. Sherry, *Acc. Chem. Res.* **2003**, *36*, 783–790.
[36] B. Hamelin, L. Jullien, F. Guillo, J.-M. Lehn, A. Jardy, L. De Robertis, H. Driguez, *J. Phys. Chem.* **1995**, *99*, 17877–17885.
[37] A. D. Sherry, J. Ren, J. Huskens, E. Brücher, É. Tóth, C. F. G. C. Geraldes, M. M. C. A. Castro, W. P. Cacheris, *Inorg. Chem.* **1996**, *35*, 4604–4612.
[38] F. Avecilla, J. A. Peters, C. F. G. C. Geraldes, *Eur. J. Inorg. Chem.* **2003**, 4179–4186.
[39] C. F. C. G. Geraldes, A. D. Sherry, G. E. Kiefer, *J. Magn. Reson.* **1992**, *97*, 290–304.
[40] W. Saenger, J. Jacob, K. Gessler, T. Steiner, D. Hoffmann, H. Sanbe, K. Koizumi, S. M. Smith, T. Takaha, *Chem. Rev.* **1998**, *98*, 1787–1802.
[41] a) M. Botta, *Eur. J. Inorg. Chem.* **2000**, 399–407; b) J. H. Freed, *J. Chem. Phys.* **1978**, *68*, 4034–4037.
[42] a) J. Kowalewski, L. Nordenskiold, N. Benetis, P.-O. Westlund, *Prog. Nucl. Magn. Reson. Spectrosc.* **1985**, *17*, 141–185; M. Lindgren, A. Laaksonen, P.-O. Westlund, *Phys. Chem. Chem. Phys.* **2009**, *11*, 10368–10376.
[43] a) E. Belorizky, P. H. Fries, L. Helm, J. Kowalewski, D. Kruk, R. R. Sharp, P.-O. Westlund, *J. Chem. Phys.* **2008**, *128*, 052315-1-17; b) I. Bertini, J. Kowalewski, C. Luchinat, T. Nilsson, G. Parigi, *J. Chem. Phys.* **1999**, *111*, 5795–5807; c) L. Helm, *Prog. NMR Spectrosc.* **2006**, *49*, 45–64.
[44] a) S. Aime, D. Delli Castelli, E. Terreno, *Angew. Chem.* **2003**, *115*, 4665; *Angew. Chem. Int. Ed.* **2003**, *42*, 4527–4529; b) S. Aime, M. Botta, S. G. Crich, E. Terreno, P. Anelli, F. Uggeri, *Chem. Eur. J.* **1999**, *5*, 1261–1266.
[45] H. Lahrech, A.-T. Perles-Barbacaru, S. Aous, J.-F. Le Bas, J.-C. Debouzy, A. Gadelle, P. H. Fries, *J. Cereb. Blood Flow Metab.* **2008**, *28*, 1017–1029.
[46] J. Boger, R. J. Corcoran, J.-M. Lehn, *Helv. Chim. Acta* **1978**, *61*, 2190–2218.
[47] I. Lazar, D. C. Hrncir, W. D. Kim, G. E. Kiefer, A. D. Sherry, *Inorg. Chem.* **1992**, *31*, 4422–4424.
[48] a) G. Brunisholz, M. Randin, *Helv. Chim. Acta* **1959**, *42*, 1927–1938; b) A. Barge, G. Cravotto, E. Gianolio, F. Fedeli, *Contrast Media Mol. Imaging* **2006**, *1*, 184–188.
[49] P. K. Glasoe, F. A. Long, *J. Phys. Chem.* **1960**, *64*, 188–189.
[50] R. Dennington, T. Keith, J. Millam, *GaussView*, version 5, Semichem Inc., Shawnee Mission, KS, USA, **2009**.
[51] *Micromath Scientist*, version 2.0, Salt Lake City, Utah, USA, **1998**.
[52] *OriginPro*, version 7.5 SR0, Northampton, MA 01060, USA, **2007**.

Received: October 28, 2011
Published Online: February 13, 2012

